

Experimental summary on global observables, hadron spectra and ratios

Thomas S. Ullrich ^a

^a Brookhaven National Laboratory, Upton New York 11973-5000, USA

1. Introduction

In this article I summarize results on global observables, hadron spectra, and ratios of integrated hadron yields as presented at the Quark Matter 2002 Conference. I also attempt to put these results into context and convince the reader that an evolving coherent picture begins to form, shedding light on the state of matter created in relativistic heavy ions collisions. However, at this conference we have been presented with such a wealth of new data on hadronic signals that no summary can give proper credit to everyone. A definitive summary of all the results on hadron spectra, ratios, and yields and their interpretation would certainly require a much longer paper. I therefore limit myself to a compilation of results that I consider to be the most interesting, and refer the reader to the large number of excellent papers given at the conference for further details.

It was obvious that this conference was dominated by the latest findings from the RHIC experiments. Despite the short time span between the last run and the Conference, spectra of many particle species were reported, both over a wide range in p_T and, for the first time, also systematically over a broad range of rapidity. The longer RHIC run in 2001/2002, delivering for the first time the design energy of $\sqrt{s_{NN}} = 200$ GeV, allowed the experiments to accumulate more statistics and, together with the progress in the understanding of the detectors, resulted in higher precision measurements than possible at the lower energy ($\sqrt{s_{NN}} = 130$ GeV) studied in the previous run in 2000/2001.

Although the SPS heavy ion program at CERN has been almost completed, with all experiments delivering the physics they were built for, work on the analysis of data, their systematic comparison and interpretation continues. In order to understand the physics behind the state of matter produced in relativistic heavy ion collisions one must, more than everything else, understand the excitation functions of all observables involved. Only if we are able to describe the evolution and behavior of the systems as we increase the energy – from AGS, through SPS to RHIC – will we gain insight into the rich variety of physics we are facing.

In this article I start with a summary of global observables presented at this conference followed by a discussion of particle ratios and chemical freeze-out conditions. I then address the question of boost-invariance at RHIC and conclude with a discussion of transverse momentum spectra and kinetic freeze-out parameters.

2. Global Observables

One of the earliest probes suggested for QGP formation involves a study of the global parameters of the events, e.g. the energy deposition, multiplicity, and the average transverse momentum of the emitted particles, as a function of center-of-mass energy $\sqrt{s_{NN}}$, mass number A , and centrality of the collision. For example, by studying the multiplicity of the produced particles one might estimate theoretically the entropy produced in the collision. Sudden changes in behavior with varying centrality or A would be indicators of a phase transition. So far, however, no such anomalous changes have been observed, at either the AGS, SPS, or RHIC. All results on global observables shown at this conference indicate a rather smooth evolution in centrality and $\sqrt{s_{NN}}$. This, of course, does not necessarily imply the absence of a phase transition, but might be rather an indication of either the insensitivity of these observables to the early phase of the collision and/or might suggest a second order phase transition (or a cross-over).

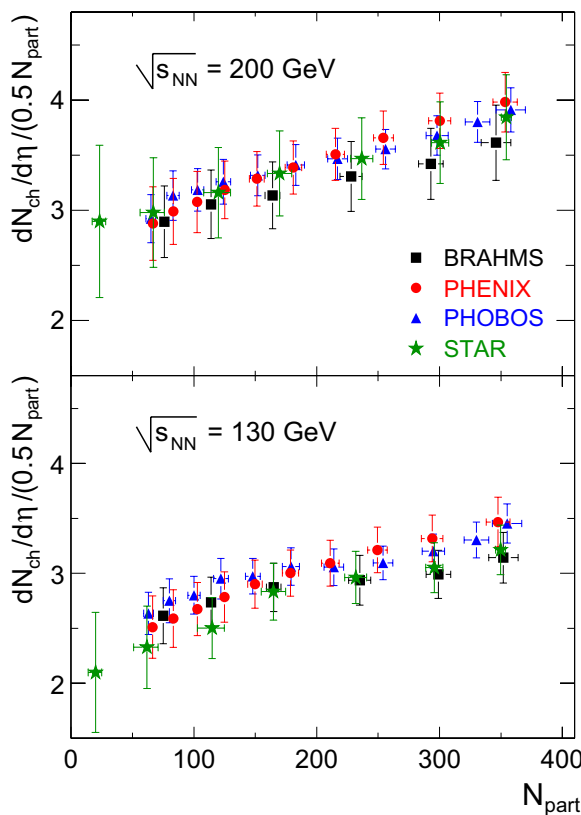


Figure 1: Charged particles per participant pair as a function of number of participants for $\sqrt{s_{NN}} = 130$ and 200 GeV for all four RHIC experiments (from [1,2]). PHENIX and STAR data are preliminary.

With the commencement of the RHIC program the question of multiparticle production in nuclear collisions became more complex due to the poorly understood role of perturbative QCD (hard processes).

The study of charged particle multiplicity as a function of the number of participants was conducted by all four RHIC experiments and the results presented in Fig. 1 depict the high quality and agreement between the experiments [1]. It should be noted that, even more than in the determination of the multiplicity and the required corrections for decays, absorption, and feed-down, the difficulties of this analysis lie in the determination of N_{part} , *i.e.* the extraction of the underlying collision geometry from the data. This requires a detailed understanding of the trigger, especially trigger efficiencies, contamination and the study of possible auto-correlations. All four RHIC experiments now use Monte-Carlo Glauber model calculations similar to the ones implemented in the Hijing model as compared to numerical calculations of the nuclear overlap

functions in the optical limit; both approaches disagree slightly, with the latter having problems estimating the total inelastic cross-sections. For the ratio of multiplicities at mid-rapidity between the two energies, $\sqrt{s_{NN}} = 200$ GeV and 130 GeV, the experiments report values of 1.14 ± 0.05 (PHOBOS & BRAHMS), 1.22 ± 0.08 (STAR), and 1.17 ± 0.03 (PHENIX) with no indication of any significant centrality dependence [1,3,4,5].

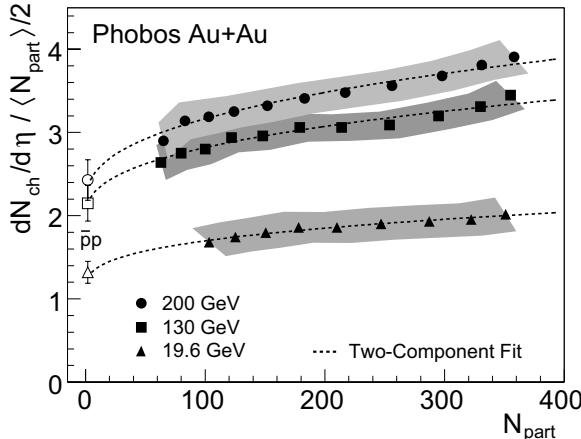


Figure 2: Charged particles per participant pair as a function of number of participants in $\sqrt{s_{\text{NN}}} = 19.6, 130$ and 200 GeV Au+Au collisions measured by PHOBOS (from [3]). The curves are two-component fits described in the text and in [6].

parametrized dependence of the saturation scale Q_s on \sqrt{s} and impact parameter allows one to predict $dN_{\text{ch}}/d\eta$. However, the predictions from these and related models have been found to be almost indistinguishable when applied to RHIC data, especially because of the large experimental uncertainties in the calculation of N_{part} for very peripheral collisions, the region where the differences between the various models become more apparent. An exception are models based on final state saturation who significantly over-predict the yield at low N_{part} . The systematic uncertainties in N_{part} for peripheral events can only be reduced when data from collisions of light ions, $A < 100$, become available.

A very surprising finding in the context of particle production was presented by the PHOBOS collaboration at this conference [3,10]. The authors noted that the total charged multiplicity per participant in elementary e^+e^- and central AA collisions is identical over a wide range of \sqrt{s} . That alone is a very remarkable fact but they also found that the same holds for the pp ($p\bar{p}$) collisions *when* compared to the effective center-of-mass energy $\sqrt{s_{\text{eff}}}$, that is the nominal energy minus the energy carried away by the leading protons. The authors actually used $\sqrt{s_{\text{eff}}} = \sqrt{s}/2$ which was verified by PYTHIA simulations. This is depicted in Fig. 3. Also shown is a perturbative QCD calculation for the multiplicity in e^+e^- fit to the data.

The agreement between the three fundamentally different collision systems is remarkable, with the exception of AA collisions below $\sqrt{s_{\text{NN}}} = 20$ GeV and pp collisions above

The interpretation of the scaling of the multiplicity at mid-rapidity as a function of N_{part} appears still ambiguous. A simple model by Kharzeev and Nardi (KN) explains the dependence in a two-component approach differentiating between soft processes scaling with N_{part} and hard processes scaling with N_{bin} [6]. When fit to the data as shown in Fig. 2 by the PHOBOS collaboration the model allows one to extract the fraction of particles produced from hard processes and one obtains values of 36% for $\sqrt{s_{\text{NN}}} = 130$ GeV, and 45% for 200 GeV, respectively [3,7]. A second class of calculations is based on parton saturation [8,9]; since the parton densities in the initial stage of the collision can be related to the density in the final state a

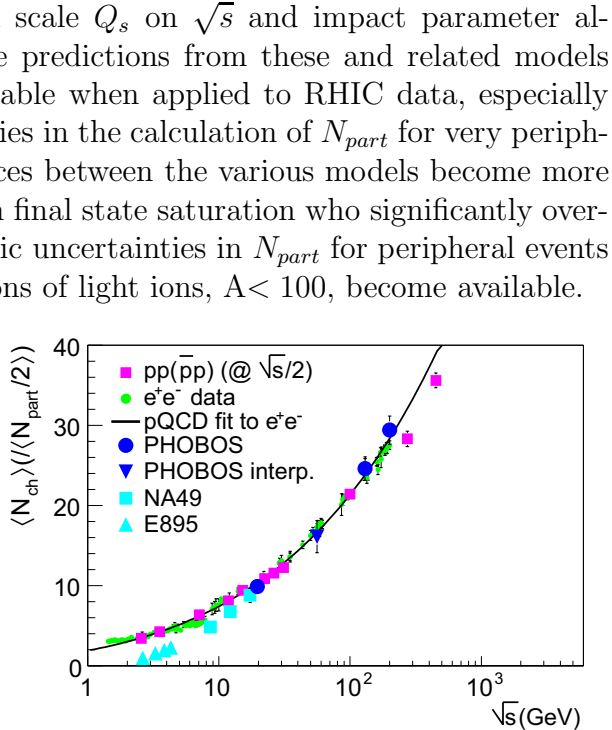


Figure 3: Total charged multiplicity per participant pair as a function of \sqrt{s} for e^+e^- , pp ($p\bar{p}$), and AA collisions. The pp ($p\bar{p}$) data is plotted versus $\sqrt{s_{\text{eff}}} = \sqrt{s}/2$ (from [10]).

200 GeV. One might speculate if this agreement is plainly accidental or if it possibly points to a kind of universality in the production of multihadronic final states in high energy collisions of *any* elementary particles over some range in \sqrt{s} . It is even more surprising that this should also apply for heavy ion collisions where we have indications that the system thermalizes and evolves on a time scale significantly larger than in elementary collisions and where the majority of particles are formed late. In comparison, the hadron production in e^+e^- is mostly from hard gluon radiation (2-,3-and 4-jet events), while in pp one observes a mixture of soft and hard processes.

To shed more light on this apparent similarity it is instructive to look at the scaling of the average transverse momentum of the produced particles in all three systems with \sqrt{s} [12]. Any universality in the production mechanism should, to some degree, also manifest itself in the evolution of $\langle p_T \rangle$. However, this seems not to hold as illustrated in Fig. 4 [5]. The figure shows that the \sqrt{s} dependence of $\langle p_T \rangle$ in e^+e^- is considerably steeper than in pp ($p\bar{p}$), mainly due to the absence of soft processes in e^+e^- collisions. This suggests that the agreement in particle multiplicity might be accidental. Still, the fact remains that the total multiplicity per participant appears to be remarkably similar for e^+e^- , nucleon-nucleon, and nucleus-nucleus collisions and further studies might help to gain insight into multihadron production in high energy collisions.

Another interesting finding depicted in Fig. 4 is the relatively small increase of $\langle p_T \rangle$ between $\sqrt{s_{NN}} = 130$ and 200 GeV of only $\sim 1\%$, as pointed out by the STAR collaboration [5]. Gluon saturation models and hydrodynamics predict a considerably stronger dependence, usually $\langle p_T \rangle^2 \propto dN_{ch}/d\eta$. The solid curve is a prediction based on the saturation model, constraint by pp ($p\bar{p}$) results [12]. The 200 GeV data point clearly falls below this prediction suggesting a flattening of the $\langle p_T \rangle$ energy dependence at RHIC. The difference is significant since the systematic errors for the 130 and 200 GeV data points are correlated. However, in order to prove or falsify any model it is essential to perform further measurements at energies between 20 and 200 GeV to study the scaling of $\langle p_T \rangle$ in greater detail.

Another important observable for characterizing the global properties of bulk matter is the transverse energy E_T . This was studied in detail by the PHENIX collaboration for $\sqrt{s_{NN}} = 130$ and 200 GeV [1] in the mid-rapidity region. They find that $dE_T/d\eta$ and $dN_{ch}/d\eta$ increase with N_{part} in a very similar fashion resulting in an almost constant ratio $\langle E_T \rangle / \langle N_{ch} \rangle \sim 0.9$ GeV. This holds for $\sqrt{s_{NN}} = 130$ and 200 GeV. Even more surprising

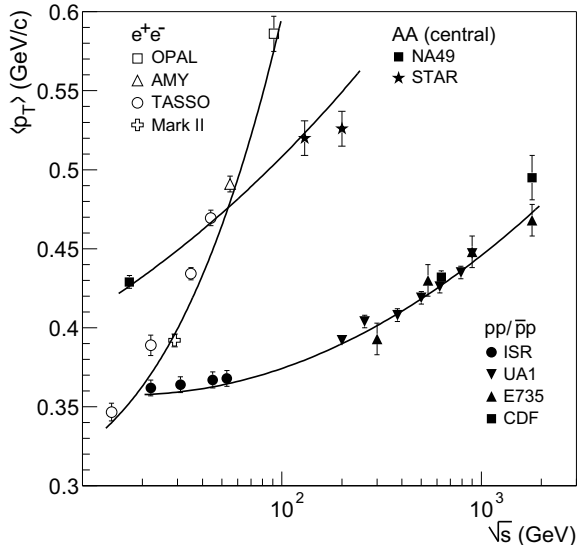


Figure 4: Mean transverse momentum versus \sqrt{s} for e^+e^- , pp ($p\bar{p}$), and AA collisions (from [5,11]). In e^+e^- the $\langle p_T \rangle$ is measured with respect to the thrust axis. The curve through the e^+e^- data points are JETSET predictions, the curve through the AA data (NA49 and STAR at 130 GeV) is from CGC predictions (see text), and that through the pp ($p\bar{p}$) data is a phenomenological parameterization in $\log(\sqrt{s})$.

is the fact that studies from Au+Au collisions at $\sqrt{s_{NN}} = 4.8$ and Pb+Pb collisions at 17.2 GeV yield very similar values, suggesting that the increased energy put into the system results solely in an increased particle production leaving the average energy per particle almost constant. This is depicted in Fig. 5. From the measured $dE_T/d\eta$ for the 2% most central Au+Au collisions at 200 GeV the authors estimated the Bjorken energy density to be $\varepsilon_{BJ} \approx 5.5$ GeV/fm³, assuming a conservative formation time of $\tau = 1$ fm/c. Similar studies at SPS in Pb+Pb collisions at $\sqrt{s_{NN}} = 17.2$ GeV give $\varepsilon_{BJ} \approx 3.2$ GeV/fm³ [13]. These values represent of course only a lower limit for the initial energy density since the longitudinal expansion of the system reduces the transverse energy considerably. Recent lattice results on QCD thermodynamics estimate the critical energy density to be $\varepsilon \approx 0.70 \pm 0.35$ GeV/fm³ [14], a value significantly surpassed already at SPS.

It is interesting to compare the scaling of $\langle E_T \rangle / \langle N_{ch} \rangle$ with that of $\langle p_T \rangle$ depicted in Fig. 4. While the small increase in $\langle p_T \rangle$ between $\sqrt{s_{NN}} = 130$ and 200 GeV is reflected by the corresponding $\langle E_T \rangle / \langle N_{ch} \rangle$ remaining constant, the considerably lower value of $\langle p_T \rangle$ at CERN/SPS energies appears to be contradicted by the transverse energy per particle. This, however, could be accounted for by the different particle composition at SPS and RHIC, although it still needs to be verified in quantitative studies. It is intriguing to compare the universality in $\langle E_T \rangle / \langle N_{ch} \rangle$ with an observation presented in a paper by Cleymens and Redlich in 1998 [15] in which the authors show that the chemical freeze-out parameters obtained at SPS, AGS, and SIS all correspond to a unique value of ~ 1 GeV for the average energy per hadron in the local rest frame of the system independent of beam energy and mass number. From what we have learned so far this empirical observation holds still at RHIC energies leading to a considerable unification in the description of hadronic final states in high energy nuclear collisions.

3. Particle Ratios and Chemical Freeze-Out

One of the most important issues in the physics of heavy ion collisions is the question if, and if so at what stage, the produced system thermalizes and to what extent a thermal description is appropriate for the evolving system. In order to discuss an equation of state and a true order to any associated phase transitions, we need to describe the system in terms of a few thermodynamic properties. The use of thermodynamic concepts to describe multi-particle production has a long history beginning with Hagedorn in the early 1960's [16]. The concept of a *temperature* applies, strictly speaking, only to systems in at least local thermal equilibrium. Thermalization is normally only thought to occur

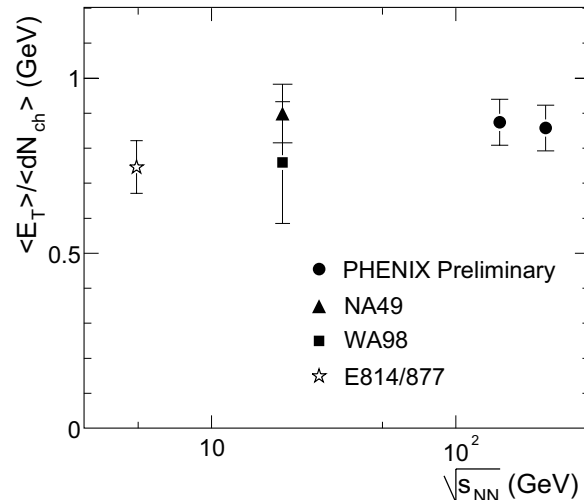


Figure 5: $dE_T/d\eta|_{\eta=0}/dN_{ch}/d\eta|_{\eta=0}$ versus $\sqrt{s_{NN}}$ for 5% most central events at AGS, SPS, and RHIC (from [1]).

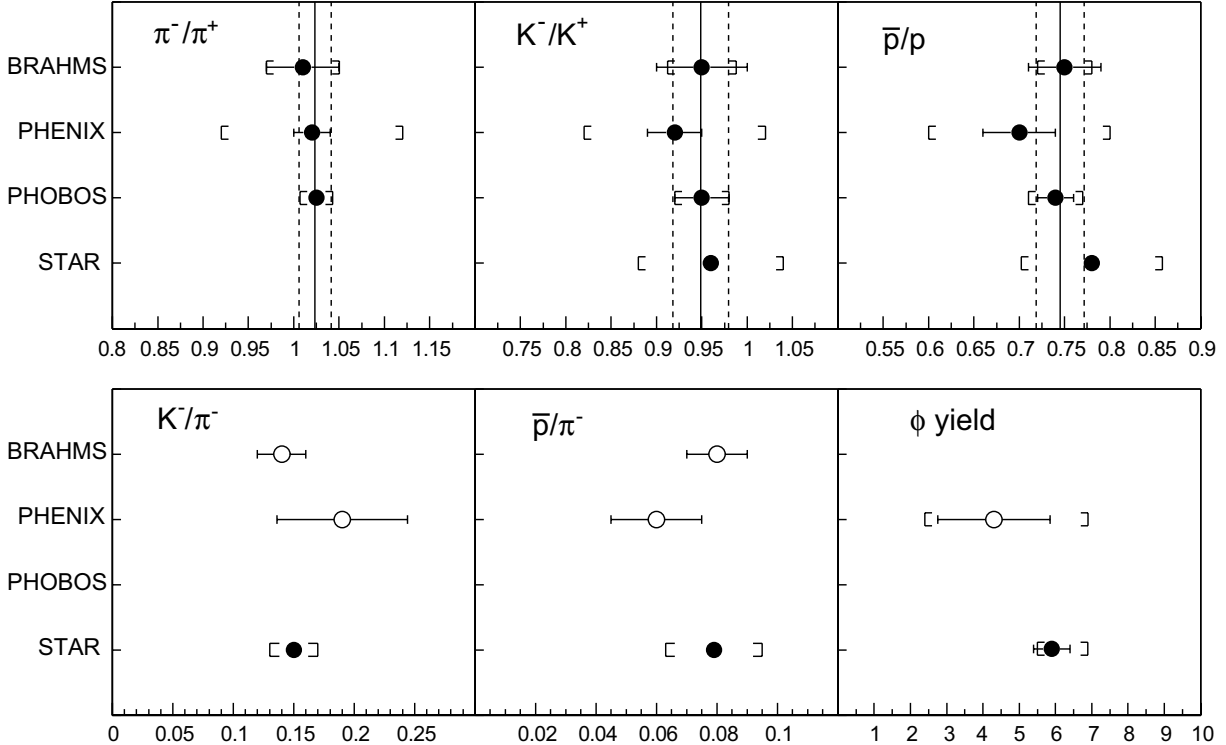


Figure 6. Particle ratios for 200 GeV central Au+Au collisions at RHIC [4,17,18,19,20,21,22]. The error bars depict the statistical errors, the brackets the systematic uncertainties. In the upper row the vertical solid lines indicate the RHIC average, the dashed lines the error on the mean. Open circles are used for data points which were extracted from figures. Results are preliminary, except BRAHMS and PHOBOS data in upper row.

in the transverse degrees of freedom as reflected in the Lorentz invariant distributions of the particles. The measured hadron spectra contain two pieces of information: (i) their normalization, *i.e.* their yields and ratios, provide the chemical composition of the fireball at the chemical freeze-out point and (ii) their transverse momentum spectra which provide information about thermalization of the momentum distributions and collective flow. It is obvious that the observed single particle spectra do not reflect earlier conditions, *i.e.* the hot and dense deconfined phase, where chemical and thermal equilibrium may have been established, since rescattering erases most traces from the dense phase. Only those effects which are accumulative during the expansion, such as flow, remain.

The assumption of a locally thermalized source in chemical equilibrium can be tested by using statistical thermal models to describe the ratios of various emitted particles. This yields a baryon chemical potential μ_B , a strangeness saturation factor γ_s , and the temperature T_{ch} at chemical freeze-out. Because of the absence of any dynamic assumptions many details can never be fully absorbed by these models. Discrepancies between model and data up to 30% should be considered inside the systematic uncertainty of the thermal model approach [23]. So far these models are remarkably successful in describing particle ratios at SPS [24,25] and now also at RHIC [26,27]. This observation, together with the large collective flow (radial and elliptic) measured at RHIC, is generally considered a strong hint that chemical equilibrium is indeed reached. The wide reaching implications

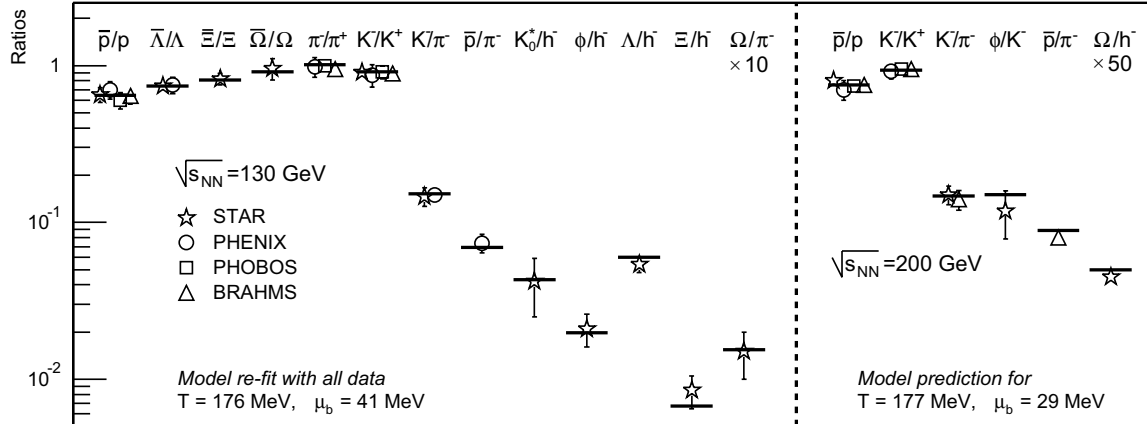


Figure 7. Left panel: comparison between RHIC experimental particle ratios for $\sqrt{s_{NN}} = 130$ GeV and statistical model calculations with $T_{ch} = 176$ MeV and $\mu_B = 41$ MeV (from [26,30]). Right panel: comparison between RHIC ratios at $\sqrt{s_{NN}} = 200$ GeV and prediction discussed in the text (also [26,30]).

of thermal statistical models and the models themselves were the subject of a dedicated podium discussion at the conference. I'm not going to summarize the issues brought up in this discussion but rather will concentrate on the recent experimental results on particle ratios and their implications in the framework of the models.

Figure 6 shows a compilation of most results on particle ratios at mid-rapidity for $\sqrt{s_{NN}} = 200$ GeV presented at the conference [4,17,18,19,20,21,22]. Given the good agreement among the experiments for the identical particle ratios and the high level of quality of the data, it is tempting to calculate the RHIC averages for these results. Adding the statistical errors and the systematical uncertainties in quadrature to derive the weights one obtains: $\pi^-/\pi^+ = 1.02 \pm 0.02$, $K^-/K^+ = 0.95 \pm 0.03$, and $\bar{p}/p = 0.75 \pm 0.03$. All experiments reported to observe no p_T or centrality dependence of these ratios for $p_T < 3$ GeV/c, confirming earlier results at 130 GeV. STAR reports a decrease in \bar{p}/p at high p_T ; for discussion on this topic and also on the significant increase of the p/π ratios from low to medium p_T see [28,29].

The analyses on non-identical particle ratios are not as complete and in most cases the systematic uncertainties are still under evaluation. While the net-baryon chemical potential at chemical freeze-out is essentially determined by the baryon to antibaryon ratios (\bar{p}/p , Λ/Λ etc.), the non-identical particle ratios are the “thermometer” of the thermal statistical models. Because of the lack of sufficient constraints it would be therefore premature to invoke the thermal model on the 200 GeV data at this point. It is, however, instructive to compare the currently available ratios with predictions made in [26]. Here the authors used a phenomenological parametrization of μ_B , obtained from thermal parameters derived from the statistical model at lower energies in conjunction with the assumption of constant energy per particle (see above) to extrapolate to 200 GeV.

This comparison, together with the statistical model fit for 130 GeV, updated with the latest values presented at this conference is shown in Fig. 7 [30]. The predictions match well with the current results and indicate no significant change in T_{ch} but a drop in μ_B from ~ 41 MeV at $\sqrt{s_{NN}} = 130$ GeV to 29 MeV at 200 GeV. The latter value is also in agreement with calculations made by various authors at the conference using different

approaches [4,18,17]. The chemical freeze-out temperature is naturally limited by the confinement phase-transition temperature assumed to be around 175 MeV, although T_{ch} is actually not constrained in thermal model fits.

Another interesting result was reported by the BRAHMS collaboration who presented a detailed study of identical particle ratios as a function of rapidity for central events [4,19]. As shown in Fig. 8 the π^-/π^+ ratio is consistent with unity over the considered rapidity range while the K^-/K^+ ratios drops by $\sim 30\%$ at $y = 3$ from its mid-rapidity value and the \bar{p}/p ratio by $\sim 70\%$. Interestingly, all ratios remain constant for $|y| < 1$, consistent with the assumption of boost invariance around mid-rapidity (see below). From those data the authors derived a net-baryon chemical potential at $y = 3$ of $\mu_B \sim 130$ MeV within the framework of a statistical model, assuming that the particle sources in the different y regions are in local chemical equilibrium and that strangeness is locally conserved. However, to what extent a thermal interpretation at large forward rapidities is justified is subject to further studies.

4. Boost Invariance at RHIC?

Many models assume directly or indirectly that the system created in heavy ion collisions is boost invariant, *i.e.* invariant under Lorentz transformations in the beam direction. Commonly, but not correctly, one considers a system boost invariant within a given rapidity interval if the rapidity distribution dN/dy is constant within that range. Strictly speaking, however, it requires all Lorentz invariant observables to remain constant. The pseudorapidity distribution of charged particles at RHIC shows a plateau extending over almost 3 units [31]. $dN/d\eta$ distributions, however, can not be used to draw any conclusions on boost invariance because the Jacobian $\partial y/\partial\eta(p_T, \eta)$ that tends to flatten otherwise peaked rapidity distributions. The BRAHMS collaboration presented at this conference the rapidity distribution of pions, kaons, and protons and their antiparticles over 6 units of rapidity ($|y| < 3$) for Au+Au collisions at $\sqrt{s_{NN}} = 200$ GeV [4].

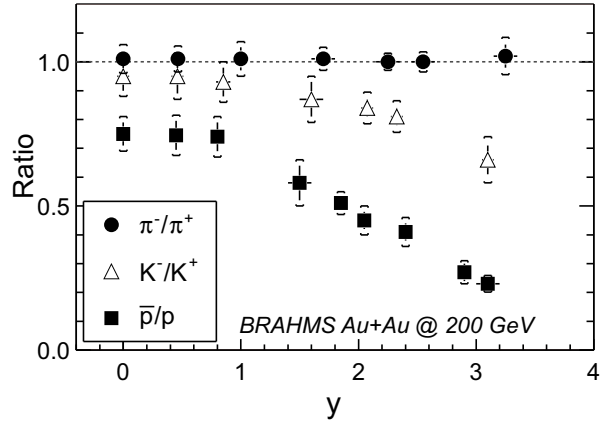


Figure 8: Antiparticle to particle ratios as a function of rapidity in 200 GeV Au+Au collisions (from [4,19]).

Figure 9: Rapidity distributions for π^\pm, K^\pm, p , and \bar{p} in 200 GeV Au+Au collisions for the top 10% most central events (data taken from [4,19]).

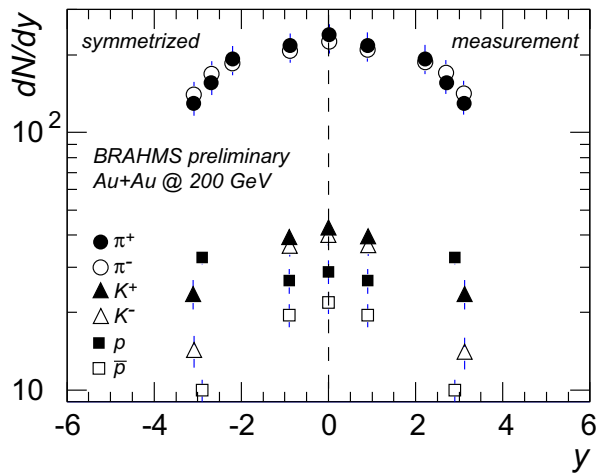


Figure 9: Rapidity distributions for π^\pm, K^\pm, p , and \bar{p} in 200 GeV Au+Au collisions for the top 10% most central events (data taken from [4,19]).

The BRAHMS collaboration presented at this conference the rapidity distribution of pions, kaons, and protons and their antiparticles over 6 units of rapidity ($|y| < 3$) for Au+Au collisions at $\sqrt{s_{NN}} = 200$ GeV [4].

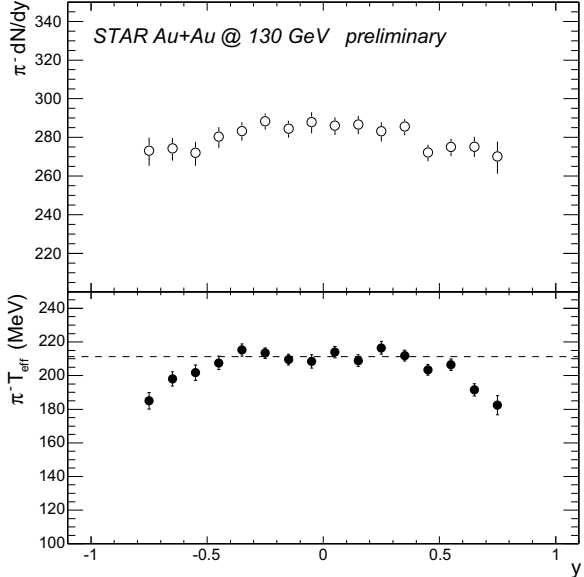


Figure 10: Upper panel: π^- rapidity distribution in 130 GeV Au+Au collisions for top 5% most central events. Lower panel: inverse slope obtained from Bose-Einstein fits to the p_T spectra at different rapidities (from [2,5]).

rapidity. Recent studies of elliptic flow also indicate a continuous drop in v_2 for $|\eta| \gtrsim 1$ that is, at least in parts, related to the strong dependence of v_2 on $p_T(\eta)$ [32]. We conclude that the currently available RHIC data suggests a rather small truly boost-invariant region of at most $|\eta| < 0.5$.

5. Inclusive Transverse Momentum Spectra and Radial Flow

Inclusive hadron spectra were intensively discussed at this conference in the context of the observed suppression of high- p_T yields for central collisions when compared to either peripheral collisions or pp ($p\bar{p}$) reference data [29]. These studies focus naturally only on a tiny fraction of all produced particles. The majority of particles emitted from the system are soft. At RHIC 99.9% of all charged particles have momenta below 2 GeV/ c , far outside the range of perturbative QCD.

Transverse momentum spectra of identified particles reflect the system at kinetic freeze-out and allow us to extract information from the latest stage of the evolution when the system was still thermally coupled and governed by elastic interactions among its constituents. The measured inverse slope parameter is determined by two components: the actual temperature at the freeze-out and the transverse flow component. In simple terms this can be approximated as $T = T_{\text{fo}} + m\langle\beta_T\rangle^2$ where β_T is the transverse flow velocity. This ansatz, however, has the disadvantage that attempts to extract T_{fo} and β_T are strongly dependent on the range in which the slopes were determined. Of even greater concern is the assumption of a fixed flow velocity which oversimplifies the problem considerably. To overcome these problems and to avoid the complexity of adjusting the initial energy density and the equation of state in a full hydrodynamical model calculation

As shown in the compilation of all six distributions in Fig. 9 and given the statistical errors and systematic uncertainties a plateau is at most limited to ± 1 unit in rapidity. The upper panel in Fig. 10 shows the pion rapidity distribution in this very region as measured by STAR with higher granularity [5]. A study of the slope of the corresponding p_T -distribution, depicted in the lower panel, shows that the slope starts to decrease from its mid-rapidity value at around $\pm\eta \sim 0.5$ thus limiting the region of boost invariance to $|\eta| < 0.5$. This is also confirmed for the case of the protons by BRAHMS where no significant change in slope is observed between $y = 0$ and 0.9 [19]. In this context it is also important to recall Fig. 8 to verify that the particle to antiparticle ratios of the most abundant particles (π , K , and p) remain constant within half a unit around mid-rapidity. Recent studies of elliptic flow also indicate a continuous drop in v_2 for $|\eta| \gtrsim 1$ that is, at least in parts, related to the strong dependence of v_2 on $p_T(\eta)$ [32]. We conclude that the currently available RHIC data suggests a rather small truly boost-invariant region of at most $|\eta| < 0.5$.

many studies now use the so-called 'blastwave' parametrization [33]. Here, the invariant cross-section is fit to

$$\frac{dN}{m_T dm_T} \propto \int_0^R r dr m_T K_1\left(\frac{m_T \cosh \rho}{T_{\text{fo}}}\right) I_0\left(\frac{p_T \sinh \rho}{T_{\text{fo}}}\right) \quad (1)$$

where $\rho = \tanh^{-1} \beta_T$ is the transverse rapidity and $\beta_T = \beta_s(r/R_{\text{max}})^n$ depends on the chosen flow profile and the flow at the surface β_s . There is no commonly accepted flow profile and n varies in the different analysis between 0.5 and 2. It is important to keep in mind that T_{fo} and β_T are correlated. Increasing T_{fo} or β_T has to some degree a similar effect on the spectral shape. This problem can be overcome by applying a blastwave motivated parametrization also to HBT radii, $R(k_T)$, since here T_{fo} and β_T are anti-correlated helping to further constrain T_{fo} and thus β_T .

Van Leeuwen presented an impressive compilation of NA49 transverse mass spectra in 40, 60, and 158 AGeV collisions [34]. Figure 11 depicts the results from Pb+Pb collisions at 158 AGeV where all spectra were fit to a blastwave parameterization. The obtained freeze-out parameters are $T_{\text{fo}} = 114 - 127$ MeV and $\langle \beta_T \rangle = 0.48 - 0.50$ in agreement with previous studies. Blastwave fits to RHIC data give a slightly smaller freeze-out temperature $T_{\text{fo}} \sim 110$ MeV but a higher flow value $\langle \beta_T \rangle = 0.55 - 0.6$ due to the higher pressure in the system [5,35]. The surprising finding in the NA49 analysis, however, is the fact that not only are the π , K , p , and Λ spectra well described by the fit but so are the spectra of the multi-strange baryons Ξ and Ω . So far multi-strange baryons were assumed to show less or no flow, due to a possibly very small elastic cross-section. This was supported by simple fits to the Ω spectra which yield T_{fo} values close to the chemical freeze-out temperature. It has been speculated that if the elastic cross-sections for the Ω were indeed very small, a non-zero flow component could be interpreted as a signature for partonic flow. The situation at RHIC is still ambiguous since the current Ω m_T -spectra lack statistics and within the errors can be fit by either assuming $T_{\text{fo}} \sim 170$ and $\langle \beta_T \rangle \sim 0.4$ or $T_{\text{fo}} = 130$ and $\langle \beta_T \rangle \sim 0.5$ [36]. One can, however, already exclude the cases of no flow and, unlike at SPS, it cannot be described by parameters obtained from fits to pions, kaons, and protons alone. To what extent a combined fit of all spectra, similar to that presented for the SPS, yields better results still has to be seen. Higher precision data is certainly needed here.

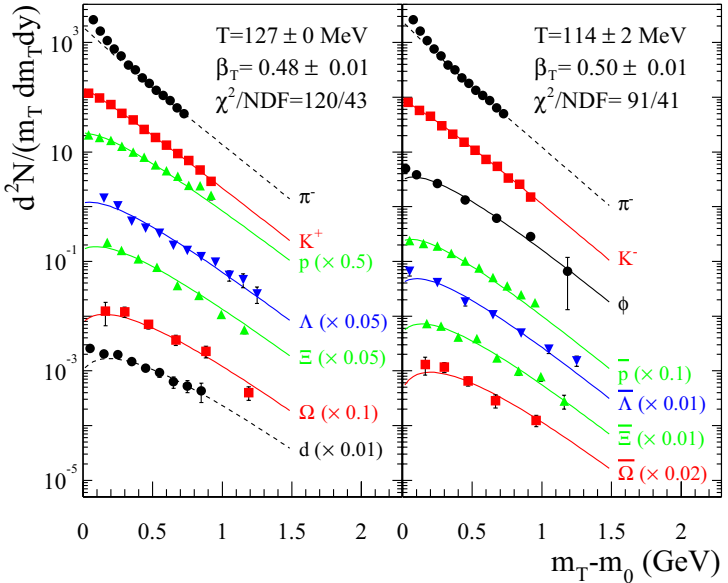


Figure 11: Transverse mass spectra in central 158 AGeV Pb+Pb collisions measured by NA49. The curves show the result of blastwave fits (from [34]).

Figure 12 shows a compilation of p_T spectra for π^- , K^- and \bar{p} from all four RHIC

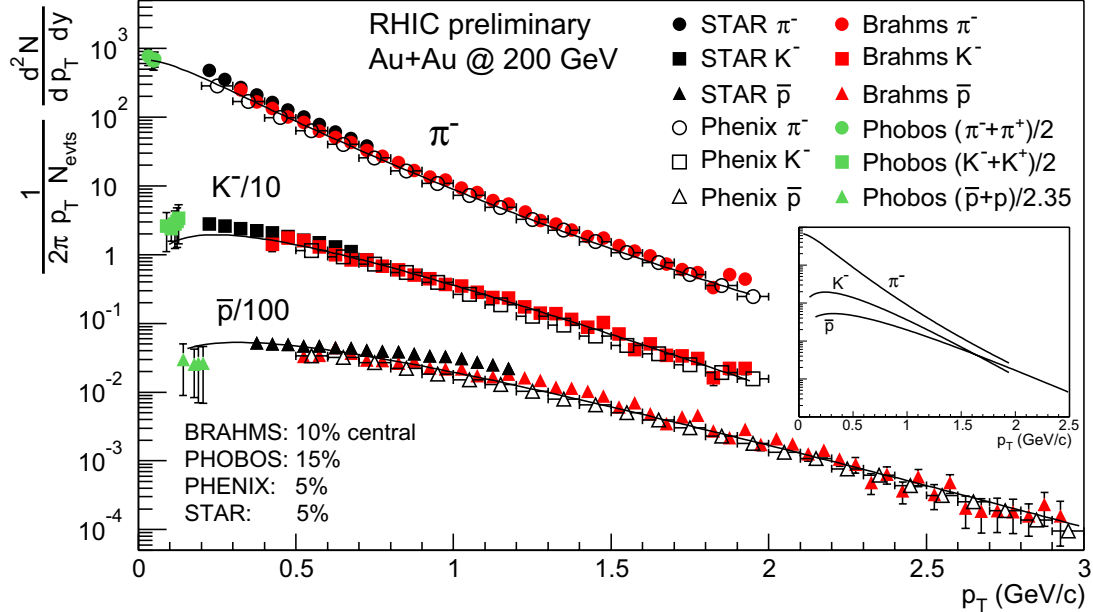


Figure 12. Compilation of preliminary transverse momentum spectra of π^- , K^- , and \bar{p} for 200 GeV central Au+Au collisions from all RHIC experiments. Except for the PHOBOS data all spectra are not feed-down corrected. The curves are fits to PHOBOS, BRAHMS, and PHENIX data. For π^- a power law in m_T was used; Maxwell-Boltzmann distributions for K^- and \bar{p} .

experiments at $\sqrt{s_{NN}} = 200$ GeV. For the first time the PHOBOS collaboration presented data at very low p_T , down to 30 MeV for pions, thus extending our knowledge into a range which is not accessible to the other three experiments. The low- p_T region is very sensitive to dynamic effects and will help to constraint models even further. Except for PHOBOS all spectra shown in the figure are not feed-down corrected. It is important to note, that the RHIC experiments are not equally sensitive to feed-down, e.g. BRAHMS because of its small aperture is less affected than a large acceptance detector such as STAR. Note, also the slightly different centrality selections. The difference in yields between 15% and 5% centrality is approximately 15%. One of the problems in determining the absolute yield of particles is the need to extrapolate to $p_T = 0$. At RHIC this results in considerable uncertainties in the yields of typically $\sim 5 - 10\%$ for experiments limited to $p_T > 200$ MeV/c or above. The new low- p_T data now allows us to significantly reduce this source of uncertainty. It is interesting to note that pion spectra actually do not follow a power-law in p_T down to low p_T as indicated by earlier measurements, but can be very well described by a power-law in m_T : $\propto A(1 + m_T/m_0)^{-n}$ as indicated by the fit shown in Fig. 12.

Radial flow affects the spectra of heavier particles considerably more than light particles. One of the consequences of strong radial flow at RHIC is that the yields of pions, kaons, and protons essentially become equal at around $p_T = 2$ GeV/c as depicted in the smaller panel in Fig. 12. At large p_T the baryon to meson ratios should drop again as flow should affect high- p_T particles to a much lesser degree and the ratios should approach values predicted by pQCD. Other studies follow a different approach, invoking novel baryon dynamics attributed to gluonic baryon junctions that predict the baryon-enhancement only in a finite moderate- p_T window [37]. However, the 'turn-over' point, predicted in these models to be around 3 GeV/c, has not yet been clearly identified [17].

6. Summary

The recent results highlighted at the conference and in this review show the enormous efforts of the community to study 'bulk' matter governed by the non-perturbative regime of QCD. The new RHIC data recorded at $\sqrt{s_{\text{NN}}} = 200$ GeV seem, without exceptions, to confirm the picture that evolved from the first data, at 130 GeV, reported at Quark Matter 2001. This picture cannot be understood in terms of global variables, ratios, and spectra alone but only by combining the information we get from studies of HBT, elliptic flow, and high- p_T , to name only a few.

Although we observe quantitative differences between SPS and RHIC in many parameters, there appears not to be any striking qualitative difference between these two energy regimes with the very prominent exception of the onset of hard scattering processes at RHIC.

The study and interpretation of soft hadron spectra, particle ratios, and yields is dominated by the success of the thermal statistical models. Although critical issues concerning these models need to be resolved, it remains a fact that they describe the ratios and yields remarkably well over a wide range of energies. They indicate that in the energy range from a few GeV up to RHIC energies the observed hadrons originate from a system in chemical equilibrium along a unified freeze-out curve. This curve provides the relation between the temperature and the baryon chemical potential. At RHIC we are approaching an almost net-baryon free system with $\mu_B \sim 25$ MeV where, for the first time, more baryons are produced at mid-rapidity than transported from beam-rapidity. The chemical freeze-out temperatures at SPS ($T_{\text{ch}} \sim 165$ MeV) and at RHIC ($T_{\text{ch}} \sim 175$ MeV) extracted from these models appear to be close to the critical temperature. This implies that chemical equilibrium is not caused by kinetic equilibration through hadronic rescattering but indicates that hadron formation proceeds by statistical hadronization from a prehadronic state.

Detailed analysis of the hadron spectra shows that the system expands collectively under strong internal pressure. Radial flow at RHIC appears to be slightly higher than at SPS, the kinetic freeze-out temperatures are very close to each other, possibly somewhat lower at RHIC ($T_{\text{fo}} \sim 110$ MeV) than at SPS ($T_{\text{fo}} \sim 120-130$ MeV). Studies of resonances [38] and correlations [39] show that the time scale for emission is very short (2-3 fm/c) while the overall lifetime of the system appears to be on the order of 10 fm/c. This implies that after hadronization the hadron abundances freeze out more or less immediately.

We could declare proof of the quark-gluon plasma on the basis of indirect evidence, but the fact that a new phase exists is almost trivial compared to characterizing its features. The interpretation of bulk properties in heavy ion collisions was, and still is, complex. We have evidence for thermalization of hot and dense matter and we have indications of unusual behavior in rare, high momentum probes. The level of collectivity is surprising but the timescales are puzzling. We observe matter that is surely not a simple collection of elementary particles, and we have the tools to study it.

Let me finally thank all the speakers at the conference who have provided me with their results. I am grateful to many colleagues for critical discussions and useful support, in particular to M. Baker, R. Bellwied, M. Calderon, H. Caines, J. Harris, B. Hippolyte, F. Laue, D. Magestro, K. Redlich, C. Suire, and Z. Xu.

REFERENCES

1. A. Bazilevski (PHENIX), these proceedings.
2. M. Calderon (STAR), conference poster and private communications.
3. M. Baker (PHOBOS), these proceedings.
4. I. Bearden (BRAHMS), these proceedings.
5. G. Van Buren (STAR), these proceedings.
6. D. Kharzeev and M. Nardi, Phys. Lett. B 507, 121 (2001).
7. B.B. Back *et al.*, Phys. Rev. C 65, 061901 (2002).
8. K.J. Eskola, K. Kajantie, and K. Tuominen, Phys. Lett. B 497, 29 (2001).
9. D. Kharzeev and E. Levin, Phys. Lett. B 523, 79 (2001).
10. P. Steinberg (PHOBOS), these proceedings.
11. R. Akers *et al.*, Phys. Lett. B 320, 417 (1994) and references therein.
12. Z. Xu (STAR), nucl-ex/0207019.
13. T. Alber *et al.*, Phys. Rev. Lett. 75, 3814 (1995).
14. F. Karsch, Nucl. Phys. A 698, 199 (2002).
15. J. Cleymans and K. Redlich, Phys. Rev. Lett. 81, 5284 (1998).
16. R. Hagedorn, Suppl. A. Nuovo Cimento Vol III, No.2 (1965) 150.
17. T. Chujo (PHENIX), these proceedings and nucl-ex/0209027.
18. B. Wosiek (PHOBOS), these proceedings.
19. J.H. Lee (BRAHMS), these proceedings.
20. F. Wang (STAR), these proceedings.
21. E. Yamamoto (STAR), these proceedings.
22. D. Mukhopadhyay (PHENIX), these proceedings.
23. U. Heinz, Nucl. Phys. A661, 140 (1999).
24. P. Braun-Munzinger, I. Heppe, and J. Stachel, Phys. Lett. B 465 (1999) 15.
25. F. Becattini *et al.*, Phys. Rev. C 64, 024901 (2001).
26. P. Braun-Munzinger *et al.*, Phys. Lett. B 518 (2001) 41-46.
27. F. Becattini, J. Phys. G 28, 1553 (2002).
28. G. Kunde (STAR), these proceedings.
29. T. Peitzmann, these proceedings and nucl-ex/0209020.
30. D. Magestro, conference poster and private communications.
31. B.B. Back *et al.*, Phys. Rev. Lett. 87, 102303 (2001).
32. S. Manly (PHOBOS), these proceedings.
33. E. Schnedermann, J. Sollfrank, and U. Heinz, Phys. Rev. C 48, 2462 (1993).
34. M. van Leeuwen (NA49), these proceedings and nucl-ex/0208014.
35. J. Burward-Hoy (PHENIX), these proceedings.
36. C. Suire (STAR), these proceedings.
37. I. Vitev and M. Gyulassy, hep-ph/0208108.
38. P. Fachini (STAR), these proceedings.
39. L. Ray (STAR), these proceedings.